Excitonic exchange splitting in bulk semiconductors

Huaxiang Fu, Lin-Wang Wang, and Alex Zunger
National Renewable Energy Laboratory, Golden, Colorado 80401
(Received 18 September 1998)

We present an approach to calculate the excitonic fine-structure splittings due to electron-hole short-range exchange interactions using the local-density approximation pseudopotential method, and apply it to bulk semiconductors CdSe, InP, GaAs, and InAs. Comparing with previous theoretical results, the current calculated splittings agree well with experiments. Furthermore, we provide an approximate relationship between the short-range exchange splitting and the exciton Bohr radius, which can be used to estimate the exchange splitting for other materials. The current calculation indicates that a commonly used formula for exchange splitting in quantum dot is not valid. Finally, we find a very large pressure dependence of the exchange splitting: a factor of 4.5 increase as the lattice constant changes by 3.5%. This increase is mainly due to the decrease of the Bohr radius via the change of electron effective mass. [S0163-1829(99)02407-8]

I. INTRODUCTION

When an electron is excited from a fully occupied valence band of a semiconductor to an empty conduction band, the electron spin can be either parallel or antiparallel to the spin of the particle (i.e., hole) left behind. This produces a fine structure of ''singlet'' and ''multiplet'' (e.g., triplet) excitons, separated by the exchange splitting.[1–5] The exchange interaction contains both a short-range (SR) part and a long-range (LR) part.[1] The short-range part can be defined in real space as the electron-hole exchange integral within a Wigner-Seitz unit cell, and the long-range part is defined as the contribution to the exchange integral coming from different cells. The exchange interaction can also be divided in k space into analytical part and nonanalytical part.[6,7] These two ways of dividing are closely related, but not exactly the same (the LR part can contain some analytical components).[6,7] We study in this paper the analytical part of the exchange splitting (but we will also use the phrase ''SR'' to mean the same thing, in a loose sense). The LR exchange splitting of bulk exciton originates from the interaction between electron-hole dipoles located at different bulk unit cells. This causes a longitudinal-transverse excitonic splitting, which further lifts the degeneracy of the excitonic multiplet state. In direct-gap zinc-blende semiconductors, for example, the eightfold degenerate $\Gamma_{8v}\rightarrow\Gamma_{6c}$ fundamental excitonic transition splits via the SR exchange interaction into a fivefold and a threefold degenerate excitons (Fig. 1). The optically active threefold degenerate exciton state will further split into doublet and singlet states via the LR exchange interaction. The measured short-range exchange splitting is subject to uncertainties due to its extremely small magnitude. This leads to a considerable spread of values. In bulk GaAs, the SR exchange splitting was measured by Gilleo *et al.* as 370 μeV using luminescence under stress;[8] by Sell *et al.* as $100\pm100\,\mu$eV using piezoreflection;[9] and by Ekardt *et al.* as $20\pm8\,\mu$eV using highly-accurate polariton spectroscopy in a magnetic field.[10] Recently, Julier *et al.*[11] measured the bulk SR exchange splitting of wurzite GaN as $600\pm100\,\mu$eV. There, they[11] also collected the values of the exchange splittings in other materials, and found that the splittings show an exponential dependence on the interatomic distance. There are only a few calculations of bulk excitonic exchange. The short-range exchange splitting was calculated by Abe[12] as 380 μeV in GaAs using variational trial functions, and by Rohner[13] as 1600 μeV in CdSe using fixed-basis diagonalization method of exchange Hamiltonian. Both results differ from the most recent respective experimental values[10,14] by more than a factor of 10.

The excitonic exchange splitting in bulk semiconductor has recently received renewed interest due to the progress made in spectroscopy of *semiconductor quantum dots*.[15–18]

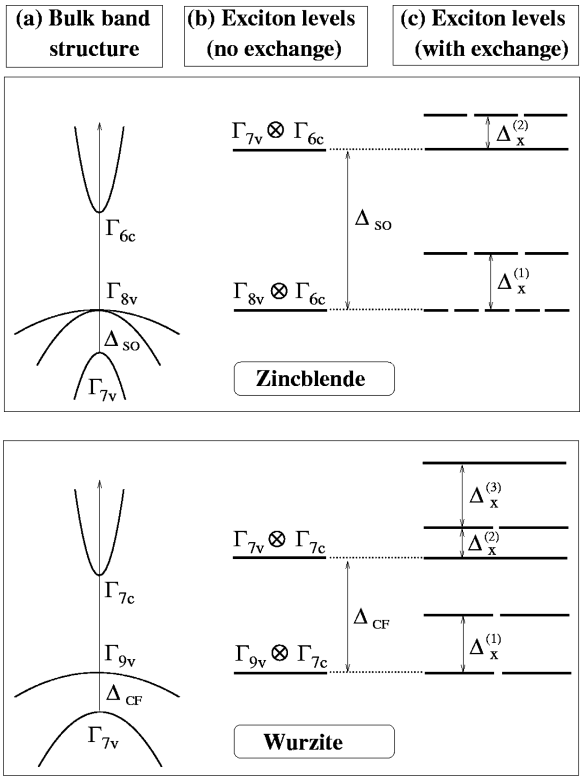

FIG. 1. Schematic illustration of (a) bulk band structure; (b) excitonic levels neglecting the exchange interaction; and (c) excitonic fine structure with exchange interaction included. In column (b), the degeneracies of two lowest exciton states are eight and four (four and four) for zinc-blende (wurzite) materials. In column (c), the number of broken horizontal lines indicates the degeneracy of excitonic level.

There, quantum confinement is expected[15] to sharply enhance the exchange interaction, leading to increased exchange splitting (>10 meV) observed as a red shift between absorption into the singlet state and emission from the lower-energy spin multiplet state. This was seen in Si,[15] CdSe,[16] InP,[17] InAs,[18] and CdS (Ref. 19) dots. In previous modeling of such a exchange splitting, the LR exchange interaction is assumed to be zero due to cancellations in a spherical quantum dot.[20,16,21] Thus, the exchange interaction in a quantum dot is represented by a SR formula:[16,18,21]

$$H_x^{\rm dot}=\frac{\Delta_x^{\rm bulk}\pi a_{\rm B}^3}{2}(\mathbf{J}_h\cdot\mathbf{J}_e)\,\delta(\mathbf{r}_h-\mathbf{r}_e), \tag{1}$$

where $\Delta_x^{\rm bulk}$ is the bulk electron-hole exchange splitting, and $\mathbf{J}_e$ ($\mathbf{J}_h$) is the total angular momentum of electron (hole), and where $a_{\rm B}$ is the Bohr radius of bulk exciton. Solving Eq. (1) under the single-band effective-mass approximation (EMA) for spherical zinc-blende semiconductor dot yields

$$\Delta_x^{\rm dot}({\rm EMA})=\Delta_x^{\rm bulk}\left(\frac{a_{\rm B}}{R}\right)^3\xi, \tag{2}$$

where R is the dot radius, and ξ is the electron-hole charge overlap. While this short-range model Hamiltonian with experimentally measured *bulk* exchange $\Delta_x^{\rm bulk}$ fits well the experimentally observed values in CdSe dots,[21] it produces incorrect R^{-3} size scaling for[17] InP (observed: $R^{-1.96}$) and[18] InAs (observed: $R^{-1.90}$).

Alternatively, the exchange interaction in dots between wave-function pairs of $\phi_{kv}^*(\mathbf{r}_h)\phi_{lc}(\mathbf{r}_e)$ and $\phi_{iv}^*(\mathbf{r}_h)\phi_{jc}(\mathbf{r}_e)$ (obtained, e.g., from pseudopotential calculations[22]) can also be calculated directly[23,24] from the exchange Hamiltonian $H_{\rm exch}$ [see Eq. (5) below] as

$$K_{kl,\,ij}^{\rm dot}=\int\int\phi_{iv}^*(\mathbf{r}_1)\;\;\phi_{lc}^*(\mathbf{r}_2)\times\frac{1}{|\mathbf{r}_1-\mathbf{r}_2|}\phi_{kv}(\mathbf{r}_2)\;\;\phi_{jc}(\mathbf{r}_1)d\mathbf{r}_1\;\;d\mathbf{r}_2. \tag{3}$$

However, we will see in the following that these two approaches [i.e., Eqs. (1) and (3)] give very different results, which implies that the basic assumption in Eq. (1) (i.e., there is only bulk-defined conventional SR exchange in dots) is not valid.

In this paper we calculate the analytical part (short-range part) of the exchange splitting of bulk exciton for zinc-blende InP, GaAs, and InAs, and for wurzite CdSe. The *ab initio* pseudopotential method in the local-density approximation (LDA) is used for the first time, to our knowledge, to obtain the bulk exciton fine structure. The spin-orbit coupling is included in the calculation. We find that our calculated bulk exchange splittings are in fair agreement with the most recent experimental values for all the considered bulk materials. The exchange splitting in quantum dots obtained from Eq. (2) using the calculated $\Delta_x^{\rm bulk}$ is found to be significantly smaller than the value obtained from direct calculation of Eq. (3). This implies that Eq. (1) is not valid in representing the total exchange interaction in a quantum dot. Finally, we predict a very large pressure dependence of excitonic exchange splitting in bulk. This result awaits future experimental testing.

II. COMPUTATION METHOD FOR THE EXCITONIC SR EXCHANGE IN BULK

The two-particle electron and hole effective Hamiltonian with Coulomb and exchange interactions can be derived[13] from many-body theory as

$$\begin{aligned}H(\mathbf{r}_1,\mathbf{r}_2;\mathbf{r}_1',\mathbf{r}_2')=&(\varepsilon_e-\varepsilon_h)\,\delta(\mathbf{r}_1-\mathbf{r}_1')\,\delta(\mathbf{r}_2-\mathbf{r}_2')\\&+H_{\rm Coul}(\mathbf{r}_1,\mathbf{r}_2;\mathbf{r}_1',\mathbf{r}_2')\\&+H_{\rm exch}(\mathbf{r}_1,\mathbf{r}_2;\mathbf{r}_1',\mathbf{r}_2'),\end{aligned} \tag{4}$$

where ε_e and ε_h are the electron and hole single-particle energies, respectively. $H_{\rm Coul}$ is the screened Coulomb interactions between electron and hole, and $H_{\rm exch}$ is the exchange interaction

$$H_{\rm exch}(\mathbf{r}_1,\mathbf{r}_2;\mathbf{r}_1',\mathbf{r}_2')=\delta(\mathbf{r}_1-\mathbf{r}_2)\,\delta(\mathbf{r}_1'-\mathbf{r}_2')\frac{1}{|\mathbf{r}_1-\mathbf{r}_1'|}. \tag{5}$$

Since we are dealing with the short-range exchange interaction, there is no screening in Eq. (5).

The general approach for the exciton problem is to diagonalize Eq. (4) directly using the electron-hole two particle wave functions. Then, the Hamiltonian includes both the Coulomb interaction $H_{\rm Coul}$, which causes the exciton binding and exchange interaction $H_{\rm exch}$. Since the effect of $H_{\rm exch}$ is much smaller than $H_{\rm Coul}$, here we will treat $H_{\rm exch}$ as a perturbation. Thus, we first solve the electron-hole two-particle system neglecting $H_{\rm exch}$ in Eq. (4). The resulting two-particle exciton wave function can be approximately represented as

$$\Psi_{iv,jc}(\mathbf{r}_h,\mathbf{r}_e)=F(\mathbf{r}_h,\mathbf{r}_e)\,\psi_{iv}^*(\mathbf{r}_h)\,\psi_{jc}(\mathbf{r}_e), \tag{6}$$

where $\psi_{iv}(\mathbf{r}_h)$ and $\psi_{jc}(\mathbf{r}_e)$ are the ith valence-band and jth conduction-band Bloch functions at the Γ point, respectively. Using an effective-mass approximation, $F(\mathbf{r}_h,\mathbf{r}_e)$ can be approximated as $f(\mathbf{r}_h-\mathbf{r}_e)\omega(\mathbf{r}_h+\mathbf{r}_e)$, where

$$f(\mathbf{r}_h-\mathbf{r}_e)=\frac{1}{\sqrt{\pi a_{\rm B}^3}}e^{-|\mathbf{r}_h-\mathbf{r}_e|/a_{\rm B}},$$

$$\omega(\mathbf{r}_h+\mathbf{r}_e)=\frac{1}{\sqrt{V}}e^{i\mathbf{k}_{ex}\cdot(\mathbf{r}_h+\mathbf{r}_e)}. \tag{7}$$

Here, V is the volume of bulk system. The excitonic Bohr radius $a_{\rm B}=\epsilon/\mu$ can be calculated from static dielectric constant ϵ and electron-hole reduced mass μ. In the following, we consider the exciton wave vector $\mathbf{k}_{\rm ex}$ being zero, which means restricting ourself to the calculation of the analytical part of the exchange splitting[6,7]

The exciton energies of $\Psi_{iv,jc}(\mathbf{r}_h,\mathbf{r}_e)$ without the exchange interaction $H_{\rm exch}$ has the degeneracy as shown in the column (b) of Fig. 1. Now, $H_{\rm exch}$ can be introduced as a perturbation to $\Psi_{iv,jc}(\mathbf{r}_h,\mathbf{r}_e)$ of Eq. (6). Thus, in a subspace rediagonalization approach, the final exciton eigenstate $\Phi^{(\alpha)}(\mathbf{r}_h,\mathbf{r}_e)$ of the Hamiltonian in Eq. (4) can be written as

$$\Phi^{(\alpha)}(\mathbf{r}_h,\mathbf{r}_e)=\sum_i^{N_v}\sum_j^{N_c} C_{iv,jc}^{(\alpha)}\Psi_{iv,jc}(\mathbf{r}_h,\mathbf{r}_e), \tag{8}$$

where $C_{iv,jc}^{(\alpha)}$ are variational coefficients of the αth excitonic state, and N_v and N_c are, respectively, the numbers of valence- (v) and conduction- (c) band basis states. The wave-function coefficients $\{C_{iv,jc}^{(\alpha)}\}$ in Eq. (8) and the excitonic energy levels $E_{\rm ex}^{(\alpha)}$ are obtained by solving the secular equation

$$\sum_i^{N_v}\sum_j^{N_c}(H_{kl,ij}-E_{\rm ex}^{(\alpha)}S_{kl,ij})C_{iv,jc}^{(\alpha)}=0, \tag{9}$$

where the elements of Hamiltonian matrix H are

$$\begin{aligned}H_{kl,ij}&=\langle\Psi_{kv,lc}(\mathbf{r}_1,\mathbf{r}_2)|H(\mathbf{r}_1,\mathbf{r}_2;\mathbf{r}_1',\mathbf{r}_2')|\Psi_{iv,jc}(\mathbf{r}_1',\mathbf{r}_2')\rangle\\&=[(\varepsilon_{jc}-\varepsilon_{iv})+E_{exciton}]\delta_{lj}\delta_{ki}+\int\int\psi_{iv}^*(\mathbf{r}_1)\psi_{lc}^*(\mathbf{r}_2)\\&\quad\times\frac{|F(\mathbf{r}_1,\mathbf{r}_1)|^2}{|\mathbf{r}_1-\mathbf{r}_2|}\psi_{kv}(\mathbf{r}_2)\psi_{jc}(\mathbf{r}_1)d\mathbf{r}_1d\mathbf{r}_2\\&=[(\varepsilon_{jc}-\varepsilon_{iv})+E_{exciton}]\delta_{lj}\delta_{ki}\\&\quad+\frac{4}{a_{\rm B}^3}{\sum_{\mathbf{G}}}'\frac{4\pi}{|\mathbf{G}|^2}\rho_{kl}^*(\mathbf{G})\rho_{ij}(\mathbf{G}).\end{aligned} \tag{10}$$

Here, $\mathbf{G}$ is the reciprocal vector of bulk lattice, and the $\mathbf{G}=0$ term should be excluded in the summation $\Sigma_{\mathbf{G}}'$. Here, $\rho_{ij}(\mathbf{G})$ is the Fourier component of $\psi_{iv}^*(\mathbf{r})\psi_{jc}(\mathbf{r})$, and the same is true for $\rho_{kl}(\mathbf{G})$. Similarly, the overlap matrix element is

$$\begin{aligned}S_{kl,ij}&=\int\int\psi_{kv}(\mathbf{r}_1)\psi_{lc}^*(\mathbf{r}_2)|F(\mathbf{r}_1,\mathbf{r}_2)|^2\psi_{iv}^*(\mathbf{r}_1)\psi_{jc}(\mathbf{r}_2)\\&\quad\times d\mathbf{r}_1d\mathbf{r}_2=\sum_{\mathbf{G}}\frac{64\pi}{[|\mathbf{G}|^2a_{\rm B}^2+4]^2}\rho_{ki}^*(\mathbf{G})\rho_{lj}(\mathbf{G}).\end{aligned} \tag{11}$$

Since the purpose of this paper is to calculate the exchange splitting, which is usually two-order of magnitude smaller than the binding energy of the exciton, the details of the Coulomb interaction are not of particular interest here. Thus, we assume in Eq. (10) that the exciton binding energy $E_{exciton}$ (including the Coulomb energy and the kinetic energy) is the same for different pairs $\{i,j\}$. The splitting obtained from Eq. (9) is the analytical (''short range'') part of the exchange interaction.

The single-particle band energies (i.e., ε_{iv} and ε_{jc}) and the wave functions (i.e., ψ_{iv} and ψ_{jc}) in Eq. (10) are calculated using first-principle LDA pseudopotential method[22] with Troullier-Martins's pseudopotential[25] and the Perdew-Zunger exchange-correlation functional.[26] We use a plane-wave basis in expanding the single-particle wave function. Typical kinetic energy cutoff of the basis set is 25 Ry, and increasing the energy cutoff to 35 Ry changes the exchange magnitude by less than 1%. The single-particle energy splittings due to spin-orbit coupling and the crystal field effects (in wurzite structure) are included in the LDA eigenvalue problem.

To calculate the Bohr radius $a_{\rm B}$ in Eq. (7), we need the effective masses of conduction band and valence band. As well known, the LDA generally underestimates the band gap, and as a result, also underestimates the effective masses. For example, the LDA-calculated hole and electron masses of bulk InP are, respectively, 0.42 and 0.057, which are smaller than the respective experimental values 0.60 (Ref. 27) and 0.077 (Ref. 28). For this reason, we calculate the excitonic Bohr radius $a_{\rm B}$ using the *experimental* effective masses and static dielectric constant ϵ. Table I (Refs. 31–41) lists all the quantities used in the calculation for excitonic Bohr radius. Note that, although the LDA results for effective masses and dielectric constants are not very accurate, the LDA wave functions are believed to be very good. This is demonstrated by comparing the LDA wave functions with the natural orbitals of the density matrix from quantum Monte Carlo calculations,[29] and with the *GW* wave functions.[30]

In comparing our current approach with previous theoretical methods,[12,13] we note the following differences: (i) Abe[12] and Rohner[13] replaced the cell-periodic part of the single-particle Bloch wave functions $\psi_{iv}(\mathbf{r})$, $\psi_{jc}(\mathbf{r})$ by unit 1. This has a dramatic effect on the final result of the exchange splitting, since as shown in Eq. (10), the exchange splitting depends crucially on the cell-periodic part of Bloch wave functions. We use instead the full wave function (including the Bloch part), as obtained in LDA pseudopotential calculations. (ii) The spin-orbit coupling is included in our approach, but ignored in previous calculations. We will see in the following (Sec. III) that the neglect of this coupling produces incorrect excitonic fine structure and artificially increases the exchange splitting.

III. THE FINE STRUCTURE OF BULK EXCITONS

Figure 1(a) illustrates schematically the bulk band structure of zinc-blende and wurzite materials, including spin-orbit coupling. For zinc-blende materials, the triply degenerate valence-band maximum (VBM) at Γ (Γ_{15v}) is split into a doubly and a singly degenerate states ($\Gamma_{8v}+\Gamma_{7v}$) due to spin-orbit coupling. In the wurzite structure, the doublet VBM (Γ_{8v}) is further split into two singlet ($\Gamma_{9v}+\Gamma_{7v}$) due

TABLE I. Measured physical quantities used in the calculations of exciton Bohr radius: lattice constant a, hole mass m_h^*, electron mass m_e^*, and static dielectric constant ϵ. The calculated exciton Bohr radius $a_{\rm B}=\epsilon/\mu$ is also given.

Material	a (Å)	m_h^*	m_e^*	ϵ	$a_{\rm B}$ (Å)
CdSe	$c=7.01$[a]	0.45[b]	0.120[b]	9.7[c]	53.98
	$a=4.30$				
InP	5.87[d]	0.60[e]	0.077[f]	12.4[g]	96.31
GaAs	5.65[h]	0.48[i]	0.067[i]	12.5[i]	112.71
InAs	6.06[j]	0.41[k]	0.023[l]	15.2[m]	368.31

[a]Reference 31.
[b]Reference 32.
[c]Reference 33.
[d]Reference 34.
[e]Reference 27.
[f]Reference 28.
[g]Reference 35.
[h]Reference 36.
[i]Reference 37.
[j]Reference 38.
[k]Reference 39.
[l]Reference 40.
[m]Reference 41.

TABLE II. Calculated spin-orbit splitting Δ_{SO}, crystal-field splitting Δ_{CF} (in units of meV), and exchange splitting $\Delta_x^{(i)}$ $(i=1,2,3)$ (in units of μeV). In this table, the available experimentally measured spin-orbit splittings, crystal-field splitting, and exchange splittings are also given in parentheses for comparison.

Material	Δ_{SO}	Δ_{CF}	$\Delta_x^{(1)}$	$\Delta_x^{(2)}$	$\Delta_x^{(3)}$
CdSe	462 (429)[a]	32 (39)[b]	49.78 ($\sim$130)[c]	18.60	59.88
InP	114 (108)[d]		18.50 (40 ± 15)[e]	9.26	
GaAs	352 (341)[f]		9.61 (20 ± 8)[e]	4.94	
InAs	370 (380)[g]		0.29	0.15	

[a]Reference 42.
[b]Reference 43.
[c]Reference 14.
[d]Reference 44.
[e]Reference 10.
[f]Reference 45.
[g]Reference 46.

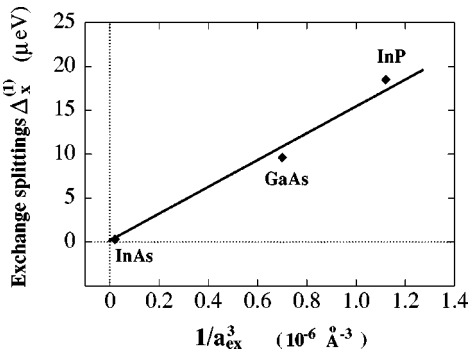

FIG. 2. Variation of the bulk exchange splitting $\Delta_x^{(1)}$ with the excitonic Bohr radius $1/a_B^3$ for zinc-blende materials InP, GaAs, and InAs, showing a linear dependence. The line is the fitted result using Eq. (12).

to the crystal field. The calculated spin-orbit splitting Δ_{SO} and crystal-field splitting Δ_{CF} are given in Table II. They agree well with experiment.[42–46]

We next study the fine structure of bulk exciton with exciton wave vector $\mathbf{k}_{ex}=0$. In the calculation of exciton fine structure for zinc-blende materials, six (counting spin degeneracy) highest valence bands $N_v=6$ (including spin-orbit split-off bands) and two lowest conduction bands $N_c=2$ are used in constructing the exciton wave functions [upper bound sum in Eqs. (8) and (9)]. For wurzite CdSe, the two spin-orbit split-off bands are not included in this basis because they are rather removed from the VBM. Including these split-off bands changes the exchange splitting by less than 0.01%. Figures 1(b) and 1(c) show schematically the excitonic energy levels obtained from solving the secular equation [Eq. (9)]. Our calculation shows that, the lowest exciton in Fig. 1(c) is fivefold degenerate in the zinc-blende structure, and twofold degenerate in the wurzite structure. The level splittings due to exchange interaction are labeled as $\Delta_x^{(i)}$ $(i=1,2,3)$ in Fig. 1(c). Table II gives the exchange splittings $\Delta_x^{(i)}$ $(i=1,2,3)$ shown in Fig. 1(c), in comparison with the available experimental data.[10,14] We see from Table II the following.

(i) Our calculated exchange splittings $\Delta_x^{(1)}$ are generally in fair agreement with experiment for different materials. Compared with previous theoretical calculations on[12] GaAs and on[13] CdSe, which gave, respectively, exchange splittings $\Delta_x^{(1)}$ of 380 and 1600 μeV, our results of 9.61 and 49.78 μeV are in much closer agreement with experimental values[10,14] 20 ± 8 and 130 μeV, respectively. We note, however, that our theoretical exchange splittings are *systematically* smaller than the experimental values. There are two possible reasons for this discrepancy: (1) We have used the pseudopotential wave functions. Had we used the all-electron wave functions, which have more large **G** components in the summation of Eq. (10) due to the rapid wave function oscillations near the nuclei. This might possibly increase our exchange splitting. (2) Since our exchange splitting is proportional to $1/a_B^3$ (see below), an experimental uncertainty of a_B by 20% may cause the error of our calculated exchange splitting by a factor of 2. To accurately describe a_B and its effect, we need to go beyond the simple model of the exciton in Eq. (7). Specifically, we need to use a $4\times4\mathbf{k}\cdot\mathbf{p}$ model to describe the exciton wave functions,[47] and to consider the local field effects on the exciton solution.[48] Considering the simple exciton model used here [Eq. (7)], our results are quite good.

(ii) For zinc-blende materials, the exchange splitting $\Delta_x^{(2)}$ originating from a hole in the split-off valence band Γ_{7v} is nearly half of the magnitude of $\Delta_x^{(1)}$, originating from a hole in valence band Γ_{8v}. If we turn off the spin-orbit coupling, the lowest exciton state in zinc-blende structure becomes ninefold degenerate, and is split from the next higher threefold degenerate exciton state. The splitting between these two levels equals the sum of $\Delta_x^{(1)}$ and $\Delta_x^{(2)}$. This indicates that the spin-orbit coupling is important to obtain realistic exchange splittings in comparison with experiments.

(iii) The magnitude of the exchange splitting decreases in the sequence of CdSe→InP→GaAs→InAs following the trend of their bulk exciton radii. Figure 2 gives the dependence of the exchange splitting $\Delta_x^{(1)}$ on $1/a_B^3$ for zinc-blende materials, which shows an almost linear relation. Fitting of the theoretical results produces

$$\Delta_x^{(1)}=15.4\times10^6/a_B^3, \tag{12}$$

where $\Delta_x^{(1)}$ is in units of μeV and a_B is in units of Å. The approximation embodied by this formula is the same as to make the result of $\Sigma_{\mathbf{G}}'$ in Eq. (10) equal for different materials. We find that the exchange splitting depends more intrinsically on the excitonic Bohr radius rather than the interatomic distance.[11] The interpolation formula [Eq. (12)] applies only to direct excitons in zinc-blende materials. For ZnTe and CdTe with a_B of 35.2 and 62.4 Å, the formula predicts $\Delta_x^{(1)}$ of 0.35 and 0.064 meV. The measured values[11] are 0.21 and 0.045 meV, respectively.

IV. IMPLICATIONS FOR QUANTUM DOTS

While the magnitude of the exciton exchange splitting in the infinite bulk solid is rather small (Table II), it is significantly enhanced in confined systems, especially in 0D quantum dots, because of the larger electron-hole wave-function overlap. As mentioned in the introduction, a widely used approach[16,18–21] is to assume only SR exchange in dots, and use Eq. (2) to calculate its amplitude. However, the validity of Eq. (2) is clouded by the fact that the bulk exchange

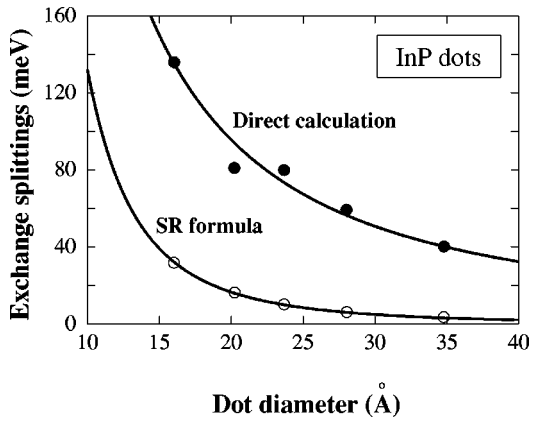

FIG. 3. The directly calculated exchange splittings in spherical InP dots (filled circles) obtained from the direct calculation [Eq. (3)] are compared with the results (open circles) obtained from the standard approach [Eq. (1)] using calculated SR bulk exchange value $\Delta_x^{\text{bulk}}=18.50\,\mu$eV. The lines are guides for the eyes.

splitting Δ_x^{bulk} is unknown in many cases. As a result, Δ_x^{bulk} is often used as a fitting parameter. For example, to fit the experimental splittings in InAs quantum dots, Banin *et al.*[18] has to use $\Delta_x^{\text{bulk}}=2.5\,\mu$eV in Eq. (1), which is unrealistically larger than our predicted value $\Delta_x^{\text{bulk}}=0.29\,\mu$eV for the same material. The main reason for this difference is the invalidity of Eq. (1) in describing the total exchange interaction in dots.

In a strong confinement dot, the exciton wave function can be written as the product of the electron and hole single-particle wave functions $\phi_{iv}^*(\mathbf{r}_h)\phi_{jc}(\mathbf{r}_e)$. As a result, the matrix element of the exchange Hamiltonian [Eq. (5)] can be calculated from Eq. (3). Note that in Eq. (3) we have neglected the dielectric screening, which might be needed for the possible long-range exchange interaction in a quantum dot.[24,49] As a result, $K_{kl,ij}^{\text{dot}}$ should not be directly compared with the experimentally observed splitting. However, if Eq. (1) is correct, then only bulk-defined conventional SR exchange exists in a spherical dot. Thus, the whole exchange interaction should not be screened. As a result, the unscreened direct calculation of Eq. (3) should have a result close to that of Eq. (2). Note that, this comparison is not obscured by the uncertainty of bulk a_{B}, which affects our results of bulk SR exchange splitting. This is because a_{B} is cancelled out when Eq. (2) is combined with Eq. (10).

We have calculated spherical InP quantum dots with up to ~1000 atoms. The single-particle dot wave functions (with spin-orbit coupling) in Eq. (3) are obtained using the LDA-derived screened atomic pseudopotential,[50] which produces greater than 99% wave-function overlap with LDA wave functions. The resulting exchange splittings from the SR formula [Eq. (2)] and from direct calculation [Eq. (3)] are shown in Fig. 3. We see that, the direct calculation results can be 10 times larger than the SR formula results,[51] for some dot sizes. This is a strong indication that the extensively used[16,18–21] short-range formula Eq. (1) is not correct in a quantum dot. In another work,[24] we have shown that there is LR exchange in spherical quantum dot, which makes Eq. (1) invalid.

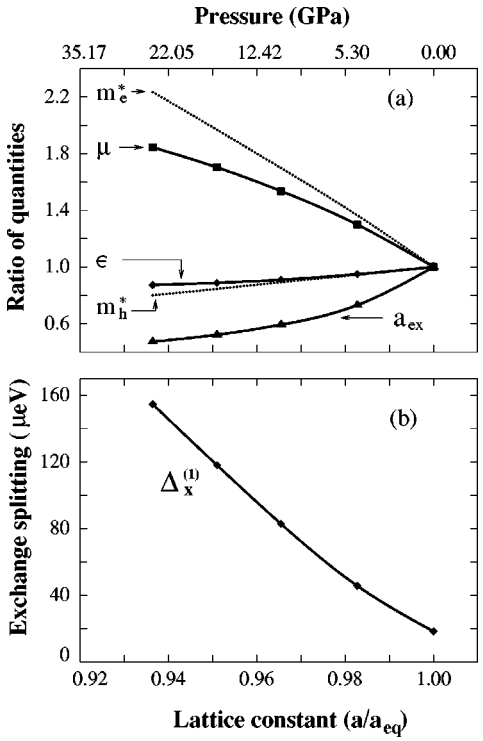

FIG. 4. Calculated pressure dependence of the following physical quantities in bulk zinc-blende InP: (a) electron mass (m_e^*), hole mass (m_h^*), reduced mass (μ), the static dielectric constant (ϵ), and the exciton Bohr radius (a_{B}). All the quantities $A(P)$ are scaled by their respective equilibrium values using $A(P)=[A_{\text{LDA}}(P)/A_{\text{LDA}}(P=0)]A_{\text{exp}}(P=0)$. (b) The resulting bulk exchange splitting $\Delta_x^{(1)}$.

V. PRESSURE DEPENDENCE OF EXCITONIC EXCHANGE IN BULK

Pressure can affect the exchange splitting since it can change not only the single-particle wave function but also the exciton Bohr radius $a_{\text{B}}=\epsilon/\mu$ by altering the e-h reduced mass μ and the static dielectric constant ϵ. To calculate the physical quantity A at pressure P, we have used $A(P)=[A_{LDA}(P)/A_{LDA}(P=0)]A_{exp}(P=0)$ to correct the LDA error. We have calculated self-consistently the bulk single-particle wave functions, effective masses and dielectric constants under different pressures using the LDA pseudopotential approach. The static dielectric constant at zero frequency $\epsilon(0)$ includes[52] both the electronic contribution $\epsilon_e(\infty)$ (which is the dominant part) and ionic contribution ϵ_{ion} [i.e., $\epsilon(0)=\epsilon_e(\infty)+\epsilon_{ion}$]. The electronic contribution $\epsilon_e(\infty)$ under different pressures is calculated from linear response theory.[53,54] The ionic contribution ϵ_{ion} is kept the same as in equilibrium volume, which is taken as the experimental value[35] 2.8 for InP.

Figure 4(a) shows how the electron mass, the hole mass, the reduced-mass, the static dielectric constant, and exciton Bohr radius in bulk InP change with pressure. Our calculation shows that the reduced mass increases dramatically with the pressure. While the dielectric constant is slightly reduced as pressure increases because of the enlarged band gap, the exciton Bohr radius shrinks significantly with the pressure. We note that the reduction of exciton radius $a_{\text{B}}=\epsilon/\mu$ is mainly due to the increase of the electron mass rather than

due to the reduced dielectric constant.

Figure 4(b) shows the exchange splitting $\Delta_x^{(1)}$ vs the pressure, demonstrating a dramatic increase. The exchange magnitude is 4.5 times of the equilibrium value when the lattice constant decreases by 3.5%. The lattice constant can be converted into pressure using the state equation:

$$B_0 + \alpha P = -V\frac{dP}{dV}, \tag{13}$$

where $B_0 = 76.0$ GPa is[55] the bulk moduli of InP at zero pressure, and $\alpha = 4.5$ is[55] the linear pressure-dependence coefficient of bulk moduli. We obtain the pressure-dependence coefficient of exchange splitting

$$\partial\Delta_x^{(1)}/\partial P = -\frac{1}{B}\partial\Delta_x^{(1)}/\partial \ln V = 6.2 \ \ \mu\text{eV/GPa}, \tag{14}$$

for bulk InP. This predicted strong enhancement of the bulk-exciton exchange splitting needs to be tested experimentally.

Since the enhancement of the bulk exchange splitting results mainly from the pressure-induced reduction of exciton radius, we expect that this pressure-induced enhancement will be absent in small dots. This expectation is based on the fact that the exciton wave function in small dots ($R < a_B$) is confined mainly by the quantum dot size (rather than by the e-h interaction), which will not be affected by the applied pressure.

VI. SUMMARY

The electron-hole exchange splitting in bulk semiconductors is studied using the first-principle pseudopotential method within the LDA scheme. The calculated exchange magnitudes agree fairly well with experiments. One formula is provided to estimate bulk exciton exchange splitting for other zinc-blende materials based on their exciton radii. This formula is quite useful since the measured exchange splitting is often not known due to its small magnitude. Our calculation indicates that the commonly used formula [Eq. (1)] for the exchange splitting in dots is not correct. Finally, the exchange splitting of bulk exciton is predicted to be strongly enhanced by the pressure mainly due to the increase of electron mass.

ACKNOWLEDGMENTS

We thank V. Ozolins for calculating the dielectric constants under different pressures, and thank A. Franceschetti, V. Ozolins, and S. H. Wei for helpful discussions. This work was supported by the U.S. Department of Energy, OER-BES, under Grant No. DE-AC36-83CH10093.

[1] R. S. Knox, Solid State Phys. **5**, 25 (1963).
[2] G. E. Pikus and G. L. Bir, Zh. Eksp. Teor. Fiz. **60**, 195 (1971) [Sov. Phys. JETP **33**, 108 (1971)]; **62**, 324 (1972) [**35**, 174 (1972)].
[3] U. Rossler and H. R. Trebin, Phys. Rev. B **23**, 1961 (1981).
[4] L. C. Andreani and F. Bassani, Phys. Rev. B **41**, 7536 (1990).
[5] E. L. Ivchenko and G. E. Pikus, *Superlattices and Other Heterostructures Symmetry and Optical Phenomena*, 2nd ed. (Springer Verlag, Berlin, 1997).
[6] K. Cho, Phys. Rev. B **14**, 4463 (1976).
[7] M. M. Denisov and V. P. Makarov, Phys. Status Solidi B **56**, 9 (1973).
[8] M. A. Gilleo, P. T. Bailey, and D. E. Hill, J. Lumin. **112**, 562 (1970).
[9] D. D. Sell, S. E. Stokowski, R. Dingle, and J. V. Dilorenzo, Phys. Rev. B **7**, 4568 (1975).
[10] W. Ekardt, K. Losch, and D. Bimberg, Phys. Rev. B **20**, 3303 (1979).
[11] M. Julier, J. Campo, B. Gil, J. P. Lascaray, and S. Nakamura, Phys. Rev. B **57**, R6791 (1998).
[12] Y. Abe, J. Phys. Soc. Jpn. **19**, 818 (1964).
[13] P. G. Rohner, Phys. Rev. B **3**, 433 (1971).
[14] V. A. Kiselev, B. S. Razbirin, and I. N. Uraltsev, Phys. Status Solidi B **72**, 161 (1975).
[15] P. D. J. Calcott, K. J. Nash, L. T. Canham, M. J. Kane, and D. Brumhead, J. Phys. C **5**, L91 (1993).
[16] M. Nirmal, D. J. Norris, M. Kuno, M. G. Bawendi, Al. L. Efros, and M. Rosen, Phys. Rev. Lett. **75**, 3728 (1995).
[17] O. I. Micic, H. M. Cheong, H. Fu, A. Zunger, J. R. Sprague, A. Mascarenhas, and A. J. Nozik, J. Phys. Chem. B **101**, 4904 (1997).
[18] U. Banin, J. C. Lee, A. A. Guzelian, A. V. Kadavanich, and A. P. Alivisatos, Superlattices Microstruct. **22**, 559 (1997).
[19] M. Chamarro, M. Dib, and V. Voliotis, Phys. Rev. B **57**, 3729 (1998).
[20] T. Takagahara, Phys. Rev. B **47**, 4569 (1993).
[21] Al. L. Efros, M. Rosen, M. Kuno, M. Nirmal, D. J. Norris, M. G. Bawendi, Phys. Rev. B **54**, 4843 (1996).
[22] J. Ihm, A. Zunger, and M. L. Cohen, J. Phys. C **12**, 4409 (1979).
[23] H. Fu and A. Zunger, Phys. Rev. B **56**, 1496 (1997).
[24] A. Franceschetti, L. W. Wang, H. Fu, and A. Zunger, Phys. Rev. B **58**, R13 367 (1998).
[25] N. Troullier and J. L. Martins, Phys. Rev. B **43**, 8861 (1991).
[26] J. Perdew and A. Zunger, Phys. Rev. B **23**, 5048 (1981).
[27] J. Leotin, R. Barbaste, and J. Tuchendler, Solid State Commun. **15**, 693 (1974).
[28] M. Helm, W. Knap, W. Seidenbush, R. Lassnig, and E. Gornik, Solid State Commun. **53**, 547 (1985).
[29] P. R. C. Kent, R. Q. Hood, M. D. Towler, R. J. Needs, and G. Rajagopal, Phys. Rev. B **57**, 15 293 (1998).
[30] M. S. Hybertsen and S. G. Louie, Phys. Rev. Lett. **55**, 1418 (1985); Phys. Rev. B **34**, 5390 (1986).
[31] R. R. Reeber, J. Mater Sci. **11**, 590 (1976).
[32] R. G. Wheeler and J. O. Dimmock, Phys. Rev. **125**, 1805 (1962).
[33] R. Geick and C. H. Perry, J. Appl. Phys. **37**, 1994 (1966).
[34] G. Giesecke and H. Pfister, Acta Crystallogr. **11**, 369 (1958).
[35] H. J. Lee, J. Basinski, L. Y. Juravel, and J. C. Wooley, Can. J. Phys. **58**, 923 (1980).
[36] J. B. Mullin, B. W. Straughan, C. M. H. Driscoll, and A. F. W.

Willoughby, IOP Conf. Proc. No. 24 (Institute of Physics, London, 1975), p. 275.
[37] J. S. Blakemore, J. Appl. Phys. **53**, R123 (1982).
[38] J. V. Ozolinsh, G. K. Averkieva, A. F. Ilvins, and N. A. Goryunova, Kristallografiya **7**, 850 (1962) [Sov. Phys. Crystallogr. **7**, 691 (1963)].
[39] L. M. Kanskaya, S. I. Kokhanovskii, R. P. Seisyan, Al. L. Efros, and V. A. Yukish, Fiz. Tekh. Poluprovodn. **17**, 718 (1983) [Sov. Phys. Semicond. **17**, 449 (1983)].
[40] J. Takayama, K. Shimomae, and C. Hamaguchi, Jpn. J. Appl. Phys. **20**, 1265 (1981).
[41] M. Hass and B. W. Henvis, J. Phys. Chem. Solids **23**, 1099 (1962).
[42] V. V. Sobolev, V. I. Donetskina, and E. F. Zagainov, Fiz. Tekh. Poluprovodn. **12**, 1089 (1978) [Sov. Phys. Semicond. **12**, 646 (1978)].
[43] O. Goede, D. Hennig, and L. John, Phys. Status Solidi B **96**, 671 (1979).
[44] J. Camassel, P. Merle, L. Bayo, and H. Mathieu, Phys. Rev. B **22**, 2020 (1980).
[45] D. E. Aspnes and A. A. Studna, Phys. Rev. B **7**, 4605 (1973).
[46] C. R. Pidgeon, S. H. Groves, and J. Feinleib, Solid State Commun. **5**, 677 (1967).
[47] A. Baldereschi and N. O. Lipari, Phys. Rev. B **3**, 439 (1971).
[48] R. Bonneville and G. Fishman, Phys. Rev. B **22**, 2008 (1980).
[49] K. Ehara and K. Cho, Solid State Commun. **44**, 453 (1982).
[50] H. Fu and A. Zunger, Phys. Rev. B **55**, 1642 (1997).
[51] This does not mean that the results from Eq. (3) can be compared with experimentally observed values. For more detailed discussion about this issue, please see Refs. 23 and 24.
[52] H. Haken, Nuovo Cimento **10**, 1230 (1956).
[53] V. Ozolins (private communication).
[54] P. Giannozzi, S. de Gironcoli, P. Pavone, and S. Baroni, Phys. Rev. B **43**, 7231 (1991).
[55] D. N. Nichols, D. S. Rimai, and R. J. Sladek, Solid State Commun. **36**, 667 (1980).